Original Article

Association between periprocedural myocardial injury and neointimal characteristics in patients with in-stent restenosis: an optical coherence tomography study

Youcheng Shen[#], Xi Wang[#], Ning Gu[#], Zhijiang Liu, Jidong Rong, Changyin Shen, Wei Zhang, Panke Chen, Yi Deng, Chancui Deng, Shuai Ma, Yongchao Zhao, Ranzun Zhao, Bei Shi

Department of Cardiology, Affiliated Hospital of Zunyi Medical University, Zunyi, China

Contributions: (I) Conception and design: Y Shen, N Gu; (II) Administrative support: B Shi, R Zhao; (III) Provision of study materials or patients: Z Liu, J Rong, C Shen, W Zhang; (IV) Collection and assembly of data: Y Deng, C Deng, S Ma, Y Zhao; (V) Data analysis and interpretation: Y Shen, X Wang; (VI) Manuscript writing: All authors; (VII) Final approval of manuscript: All authors.

[#]These authors contributed equally to this work.

Correspondence to: Ranzun Zhao, MD; Bei Shi, MD. Department of Cardiology, Affiliated Hospital of Zunyi Medical University, Dalian Road 149, Zunyi 563000, China. Email: kouke80@126.com; shibei2147@163.com.

Background: The relationship between neointimal characteristics of in-stent restenosis (ISR) and periprocedural myocardial injury (PMI) remains unclear. Therefore, this study aimed to investigate the relationship between PMI and neointimal characteristics of ISR by using optical coherence tomography (OCT).

Methods: This was a retrospective study. We enrolled 140 patients diagnosed with ISR with normal baseline high-sensitivity troponin T (hs-cTnT) levels who underwent OCT and subsequent revascularization by means of drug-coated balloon (DCB) or drug-eluting stent (DES) between October 2018 and October 2022 in the Affiliated Hospital of Zunyi Medical University. Based on the 4th universal definition of myocardial infarction, patients whose hs-cTnT were increased five times above the upper reference limit (URL) after percutaneous coronary interventions (PCI) were deemed to PMI. The patients were subdivided into PMI (n=53) and non-PMI (n=87) groups. In the univariable analysis, variables in the baselines, angiography characteristics and OCT findings were analyzed with binary logistic regression. A P value of <0.2 was included in the multivariable model. Multivariable logistic regression analysis was used to identify the independent predictors of PMI.

Results: The prevalence of intra-intimal microvessels in patients with PMI was higher than in those without PMI (58.5% *vs.* 32.2%, P=0.003). The ratio of intra-stent plaque rupture (PR) was also higher in patients with PMI (60.4% *vs.* 40.2%, P=0.021). Multivariable logistic regression analysis showed that intra-intimal microvessels [odds ratio (OR): 3.193, 95% confidence interval (CI): 1.280–7.966; P=0.013] and intra-stent PR (OR: 2.124, 95% CI: 1.153–4.732; P=0.035) were independently associated with PMI.

Conclusions: Intra-intimal microvessels and intra-stent PR were independently associated with PMI. Accurate identification and recognition of intra-intimal microvessels and intra-stent PR may be helpful in preventing PMI.

Keywords: In-stent restenosis (ISR); optical coherence tomography (OCT); periprocedural myocardial injury (PMI); intra-intimal microvessels; intra-stent plaque rupture

Submitted Oct 02, 2023. Accepted for publication Jan 05, 2024. Published online Feb 01, 2024.
doi: 10.21037/cdt-23-390
View this article at: https://dx.doi.org/10.21037/cdt-23-390

Introduction

Background

Iterations of drug-eluting stent (DES) technology have obviously decreased the frequency of in-stent restenosis (ISR), significantly improving the efficacy and safety of percutaneous coronary interventions (PCI) (1). In a nationwide registry study, the ratio of occurrence of ISR is still high (2). The current European guidelines recommend either DES or drug-coated balloon (DCB) as a Class I indication to treat ISR (3). However, not a few patients have occurred periprocedural myocardial injury (PMI).

Rationale and knowledge gap

In clinical practice, high-sensitivity troponin (hs-cTn) is used as the main biomarker for detecting myocardial injury because of its high sensitivity and specificity. PMI is defined as the increase in cardiac biomarker levels by over five-fold above the upper reference limit (URL) (4), which has been mainly reported in stable coronary artery disease (CAD) (5-7). Moreover, reports on the prognostic impact of PMI on CAD patients seemed conflicting (5-8). Previous imaging studies have investigated the association between intimal characteristics and PMI and found that thin-cap fibroatheroma (TCFA) or large necrotic cores and calcium had influence on PMI (9,10). Another imaging study explored the effect of tissue morphological characteristics of ISR on the incidence of PMI, indicating that neointimal heterogeneity, or neoatherosclerotic changes had no association with the occurrence of PMI (11).

Objective

However, there is a lack of study on the relevance of PMI and neointimal characteristics of ISR by using optical coherence tomography (OCT). Therefore, the aim of this study was to investigate the association between the occurrence of PMI and neointimal characteristics of ISR by using OCT. We present this article in accordance with the STROBE reporting checklist (available at https://cdt.amegroups.com/article/view/10.21037/cdt-23-390/rc).

Highlight box

Key findings

- Intra-intimal microvessels and intra-stent plaque rupture (PR) correlated with periprocedural myocardial injury (PMI) in patients with in-stent restenosis (ISR).

What is known and what is new?

- PMI was mainly reported in stable coronary artery disease. Previous studies have shown that intimal characteristics identified by optical coherence tomography (OCT) were associated with PMI.
- In patients with ISR, intra-intimal microvessels and intra-stent PR identified by OCT may prevent those patients from occurring PMI.

What is the implication, and what should change now?

- The study found that intra-intimal microvessels and intra-stent PR were independently associated with PMI, which may provide a strategy for the prevention of PMI.

Methods

Study population and definition

A total of 564 patients with ISR admitted to the Affiliated Hospital of Zunyi Medical University between October 2018 and October 2022 were retrospectively collected. Patients without OCT guidance (n=312), poor OCT image quality (n=5), balloon pre-dilatation before OCT examination (n=8) and absence of patients' demographic data or high-sensitivity troponin T (hs-cTnT) after PCI (n=42) were excluded. Considering that the hs-cTnT levels are time-dependent in patients with acute myocardial infarction, patients with non-ST-elevation myocardial infarction (non-STEMI) (n=34) and STEMI (n=23) were excluded. Ultimately, a total of 140 patients with 140 lesions whose baseline hs-cTnT were normal were included in the final analysis (*Figure 1*). All the 140 patients were treated with DCB or DES, which was up to the discretion of the interventional cardiologist. PMI was defined according to the criteria of the 4th universal definition of myocardial infarction (4). The patients whose hs-cTnT levels increased five times above the URL were considered as PMI. The study was conducted in accordance with the Declaration of Helsinki (as revised in 2013). The study was approved by the Ethics Committee of the Affiliated Hospital of Zunyi Medical University [No. ZMU (2022)1-177] and individual consent for this retrospective analysis was waived.

Data collection and definition

The demographic data of patients, including age, sex, coronary risk factors, laboratory data, past medicines use, time from stents implantation to ISR and underlying stent

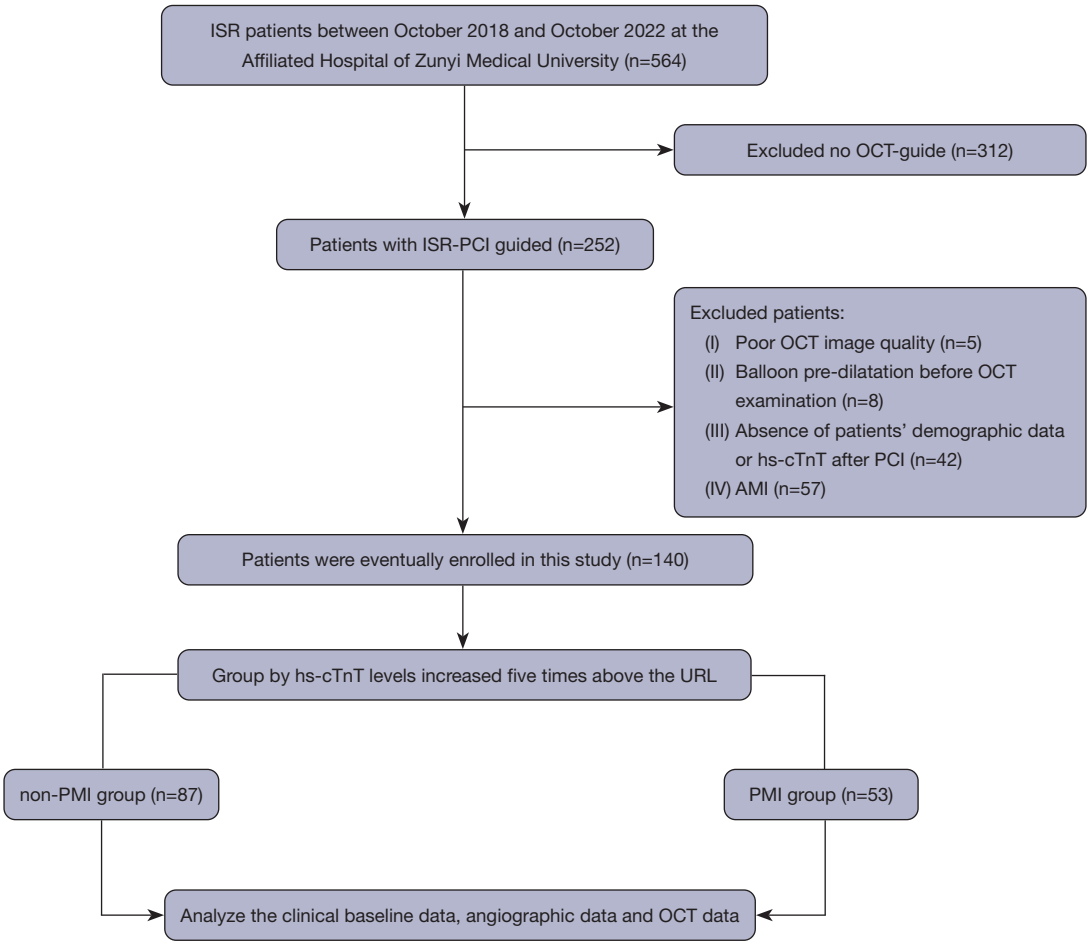

Figure 1 Study flow diagram. ISR, in-stent restenosis; OCT, optical coherence tomography; PCI, percutaneous coronary intervention; PMI, periprocedural myocardial injury; hs-cTnT, high-sensitivity troponin T; AMI, acute myocardial infarction; URL, upper reference limit.

type were collected by an experienced physician (Y.D.) between May 2022 and August 2022 from electronic medical record systems. The underlying stent type was based on the medical records provided by patients or the interventional cardiologist's estimation according to the time of stents implantation when the medical records cannot be offered. Therefore, blood samples for hs-cTnT measurements were collected in tubes containing lithium-heparin anticoagulant before the procedure (the first early morning of the patient's admission), 6 h after PCI, and on a daily basis thereafter during the hospital stay (usually 48 h). The 99th percentile URL is 14 ng/L. Baseline and peak post-procedural hs-cTnT were used for the current analysis.

For the diagnosis of hypertension, a patient must have a systolic blood pressure of ≥140 mmHg or diastolic blood pressure of ≥90 mmHg or current use of anti-hypertensive treatment. A patient diagnosed with diabetes mellitus must meet at least one of the following criteria: documented history of diabetes mellitus, use of hypoglycemic agents, fasting glucose ≥7.0 mmol/L, 2-h plasma glucose value ≥11.1 mmol/L in the 75-g oral glucose tolerance test (OGTT), classic symptom with casual plasma glucose level ≥11.1 mmol/L, or hemoglobin A1c (HbA1c) ≥6.5% (12). Dyslipidemia was defined as triglycerides level ≥1.7 mmol/L, total cholesterol (TC) level ≥5.0 mmol/L, low-density lipoprotein cholesterol (LDL-C) level ≥3 mmol/L, high-density lipoprotein cholesterol (HDL-C) ≤1.2 mmol/L, or taking medication for dyslipidemia (13). Chronic kidney disease (CKD) was defined as an estimated glomerular filtration rate (eGFR) of <60 mL/min/1.73 m^2, and the eGFR was calculated by using the 2009 Chronic Kidney Disease

Epidemiology Collaboration (CKD-EPI) equation (14).

Angiographic analysis

Coronary angiography (CAG) was performed using either the transradial or transfemoral approach, employing a 6F or 7F sheath. Coronary angiography analysis was performed using the software (Artis VC21C, Siemens AG, Berlin, Germany). Angiographic classifications of ISR were based on Mehran's classification (15), patterns of ISR were classified as type I, focal (lesions ≤10 mm); type II, diffuse in-stent (lesions >10 mm, confined to the stent); type III, diffuse proliferative (lesions >10 mm, beyond the stent edge); and type IV (total occlusion). Proximal and distal reference diameters, minimal luminal diameter, and percent diameter stenosis were calculated by an experienced physician (Z.L.) who was blinded to the clinical characteristics. All these patients were treated with DES (cobalt rapamycin DES, Shanghai Microport NeruoTech, Shanghai, China; cobalt rapamycin DES, Lepu, Beijing, China; platinum-chromium everolimus DES; Boston Scientific, Marlborough, MA, USA) or DCB (paclitaxel-coated balloon; B. Braun, Melsungen, Germany; SHENQI, Shanghai, China; Cardionovum, Grandpharma, Wuhan, China).

OCT image acquisition and analysis

A commercially available frequency-domain OCT system (C7XR, Illumien or Illumien Optis) was used to perform OCT image by an interventional cardiologist as previously described (16). Characterization of the neointimal tissue and quantitative OCT assessments of the neointima were performed at the minimal lumen area (MLA) site as well as at the five preceding and following analyzed frames. The reference site for analysis was determined as the area with the largest lumen area either proximal or distal to the stenosis. Semiautomatic measurements were performed to determine the reference lumen diameter, area of the proximal or distal site, and area stenosis (AS). The profiles of the stent and lumen were manually traced.

Neointimal tissues were categorized as homogeneous or heterogeneous. The homogeneous neointimas were characterized by high backscattering regions and no local signal attenuation. The heterogeneous neointimas were characterized by low signal regions with local signal attenuation. Lipid rich plaque (LRP) was defined as high backscattering regions with blurred edges and the fibrous caps with high-signal bands on the surface of low-signal areas. In-stent neoatherosclerosis (ISNA) was identified must meet the following criteria: macrophage infiltration and/or lipid-laden tissue within the stent or neointimal calcification (17). TCFA was defined as an LRP with the thinnest part of the fibrous cap <65 μm and an angle of lipidic tissue >180° (18). Calcification was defined as the presence of a sharp edge with a low signal or an uneven area. Cholesterol crystals were identified as thin linear area with highly backscattering regions without remarkable backward shadowing (18). Intra-stent plaque rupture (PR) was identified as the disruption of the fibrous cap with obvious cavity formation. Microvessels were defined as non-signal tubulo luminal structures without a connection to the vessel lumen recognized on more than three consecutive cross-sectional OCT images. The thrombi were categorized as red or white; a red thrombus was defined as highly backscattering region with high attenuation, and a white thrombus was defined as less backscattering and homogeneous region with low attenuation (19). Lipid length and lipid arc were measured on the longitudinal reconstructed view and the cross-sectional image, respectively. Lipid index was defined as the product of mean lipid arc multiplied by lipid length. The typical OCT images were shown in *Figure 2*. All OCT images were analyzed by an experienced physician (Z.L.) who was blinded to the clinical information, PCI procedure characteristics and angiographic findings.

Statistical analysis

Since this study was a retrospective study, the sample size was based on practical considerations. Continuous variables were presented as mean ± standard deviation (SD) for normally distributed data and were compared using independent samples *t*-test; data were expressed as median (25th–75th percentiles) when abnormally distributed and compared using the Mann-Whitney *U* test between two groups. Categorical variables were presented as number (%) and were compared using the χ^2 test or Fisher's exact test when any expected frequency of the contingency table was <5. Variables with a P value of <0.2 in the univariable analysis were included in the multivariable model. Multivariable logistic regression analysis was used to identify the independent predictors of PMI. Statistical significance was set at a two-sided P value of <0.05. Statistical analyses were performed using the SPSS version

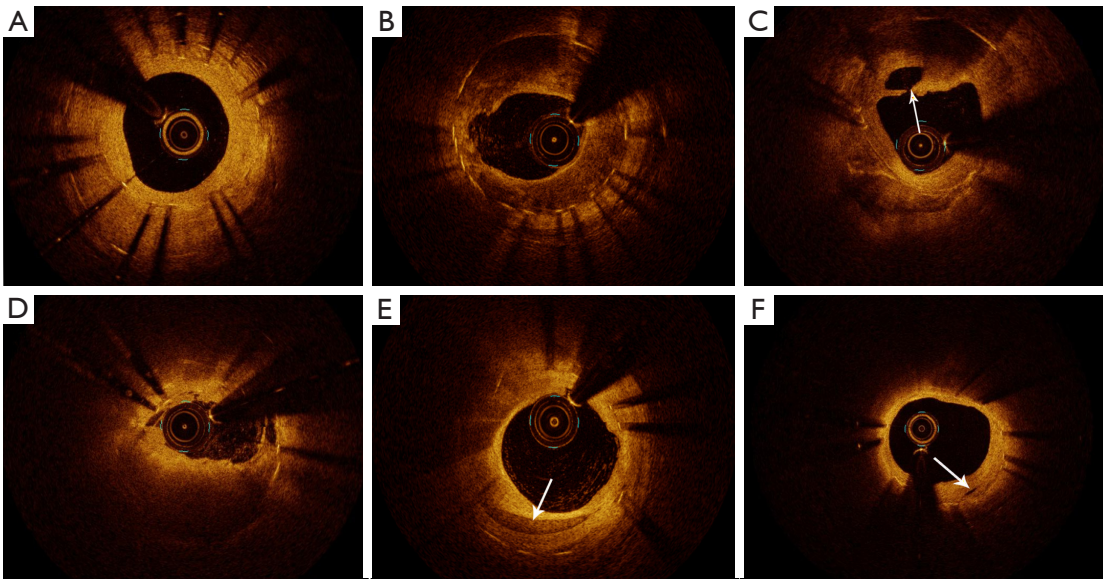

Figure 2 Representative images of optical coherence tomography findings in patients presenting with in-stent restenosis. (A) Homogeneous neointimal pattern. (B) Heterogeneous neointimal pattern. (C) Intra-stent plaque rupture (arrow). (D) Lipid-rich plaque. (E) Calcification (arrow). (F) Intra-intima microvessels (arrow).

26.0 software (IBM, Armonk, NY, USA).

Results

Clinical characteristics and angiographic findings

A total of 140 patients with 140 lesions were divided into PMI and non-PMI groups according to the definition above. Baseline clinical and angiographic characteristics are shown in *Tables 1,2*. Fifty-three patients (37.9%) encounter PMI during revascularization for ISR. A total of 116 (82.9%) men and 24 (17.1%) women were included, and the median age of the patients was 65 (57 to 72) years. The concentration of N-terminal pro-B-type natriuretic peptide (NT-proBNP) was lower in the PMI group than in the non-PMI group [281 (112.5, 1,259.0) *vs.* 133.3 (79.2, 469.0), P=0.022]. Among the 140 patients, 64 (45.7%) patients were treated with DES and 76 (54.3%) patients were treated with DCB. The prevalence of slow flow in patients with PMI was higher than those without PMI. There were no significant differences in coronary risk factors, laboratory data (except NT-proBNP levels) and angiographic findings between the two groups.

OCT findings

The OCT findings are shown in *Table 3*. Compared with the patients without PMI, those encountering PMI had a higher prevalence of intra-intimal microvessels and intra-stent PR [31 (58.5%) *vs.* 28 (32.2%), P=0.003; 32 (60.4%) *vs.* 35 (40.2%), P=0.021, respectively]. Other characteristics of OCT images were not significantly different between the two groups.

Predictors of PMI

In the overall 140 patients with ISR who underwent OCT before revascularization, the following variables with P<0.2 in the univariable analysis (Table S1) were tested: age, homogeneous neointima, heterogeneous neointima, ISNA, LRP, peri-strut microvessels, intra-intima microvessels, intra-stent plaque rupture, minimal lumen diameter (MLD), MLA, mean lipid arc, lipid length, lipid index and mean balloon length. In the multivariable logistic regression analysis, intra-intimal microvessels [odds ratio (OR): 3.193, 95% confidence interval (CI): 1.280–7.966, P=0.013] and intra-stent PR (OR, 2.124; 95% CI: 1.153–4.732, P=0.035) were independently associated with PMI (*Table 4*).

Discussion

Key findings

The main findings of this study can be summarized as

Table 1 Baseline characteristics

Variables	Total (n=140)	Non-PMI (n=87)	PMI (n=53)	P value
Age, years	65.0 (57.0, 72.0)	67.0 (58.5, 72.5)	63.0 (53.5, 72.0)	0.160
Male	116 (82.9)	71 (81.6)	45 (84.9)	0.616
LVEF, %	52.3±10.8	51.0±10.8	54.8±10.5	0.057
Heart rate	76.5±12.7	76.1±12.0	77.1±13.8	0.642
SBP, mmHg	129.4±20.0	130.9±21.3	127.0±17.7	0.263
DBP, mmHg	78.0±12.1	77.2±11.9	79.3±12.4	0.331
Coronary risk factors				
Hypertension	85 (60.7)	56 (64.4)	29 (54.7)	0.257
Diabetes mellitus	33 (23.6)	23 (26.4)	10 (18.9)	0.306
Dyslipidemia	38 (27.1)	21 (24.1)	17 (32.1)	0.306
CKD	34 (24.3)	23 (26.4)	11 (20.8)	0.447
Stroke	6 (4.3)	4 (4.6)	2 (3.8)	0.710
Smoking	68 (48.6)	43 (49.4)	25 (47.2)	0.796
Previous MI	40 (28.6)	24 (27.6)	16 (30.2)	0.741
Laboratory data				
TC, mmol/L	3.79 (3.19, 4.83)	3.73 (3.26, 5.01)	4.21 (3.46, 4.96)	0.691
Triglyceride, mmol/L	1.46 (1.16, 2.14)	1.46 (1.20, 2.58)	1.66 (1.18, 2.37)	0.253
LDL-C, mmol/L	2.15 (1.75, 2.81)	2.10 (1.82, 2.97)	2.37 (1.98, 2.90)	0.908
HDL-C, mmol/L	1.05 (0.90, 1.24)	0.98 (0.86, 1.31)	1.11 (0.99, 1.23)	0.271
FBG, mmol/L	7.15±3.18	6.89±2.80	7.55±3.69	0.291
Uric acid, μmol/L	369.0 (307.0, 468.5)	364.0 (303.0, 467.0)	371.0 (312.0, 485.0)	0.706
eGFR, mL/min/1.73 m^2	80.2±26.2	77.8±26.5	84.0±25.7	0.174
Hemoglobin, g/L	139.9±16.8	139.2±15.2	141.0±19.1	0.533
NT-proBNP, pg/mL	199.1 (92.0, 741.0)	281 (112.5, 1,259.0)	133.3 (79.2, 469.0)	0.022
Clinical presentation				0.645
Silent ischemia	28 (20.0)	18 (20.7)	10 (18.9)	
Stable angina pectoris	40 (28.6)	25 (28.7)	15 (28.3)	
Unstable angina pectoris	72 (51.4)	44 (50.6)	28 (52.8)	
Medicines at discharge				
Aspirin	103 (73.6)	66 (75.9)	37 (69.8)	0.431
P2Y12 inhibitor	46 (32.9)	30 (34.5)	16 (30.2)	0.600
B-blocker	111 (79.3)	69 (79.3)	42 (79.2)	0.993
Statin	116 (82.9)	72 (82.8)	44 (83.0)	0.968
Index stent interval, days	1,420.0 (439.8, 2,636.3)	1,590.0 (529.0, 2,737.0)	1,460.0 (497.0, 2,555.0)	0.355
Underlying stent type				
BMS	57 (40.7)	36 (41.4)	21 (39.6)	0.837
First-generation DES	53 (37.9)	31 (35.6)	22 (41.5)	0.487
New-generation DES	30 (21.4)	20 (23.0)	10 (18.9)	0.564

Data are presented as median (interquartile range), n (%), and mean ± standard deviation. PMI, periprocedural myocardial injury; LVEF, left ventricular ejection fraction; SBP, systolic blood pressure; DBP, diastolic blood pressure; CKD, chronic kidney disease; MI, myocardial infarction; TC, total cholesterol; LDL-C, low-density lipoprotein cholesterol; HDL-C, high-density lipoprotein cholesterol; FBG, fasting blood-glucose; eGFR, estimated glomerular filtration rate; NT-proBNP, N-terminal pro-B-type natriuretic peptide; BMS, bare metal stent; DES, drug eluting stent.

Table 2 Angiography characteristics

Variables	Total (n=140)	Non-PMI (n=87)	PMI (n=53)	P value
Restenosis morphology*				0.975
Type I	57 (40.7)	35 (40.2)	22 (41.5)	
Type II	40 (28.6)	24 (27.6)	16 (30.2)	
Type III	37 (26.4)	24 (27.6)	13 (24.5)	
Type IV	6 (4.3)	4 (4.6)	2 (3.8)	
Target vessel				0.854
LAD	93 (66.4)	57 (65.5)	36 (67.9)	
RCA	35 (25.0)	23 (26.4)	12 (22.6)	
LCX	12 (8.6)	7 (8.0)	5 (9.4)	
Slow flow	6 (4.3)	0	6 (11.3)	0.002
RVD (proximal), mm	3.24±0.46	3.18±0.47	3.33±0.44	0.067
RVD (distal), mm	2.50±0.56	2.57±0.53	2.40±0.60	0.074
DS, %	57.9±6.4	58.4±6.5	57.1±6.1	0.161
MLD, mm	1.44±0.31	1.41±0.32	1.49±0.31	0.262
Treatment modality				
DES	64 (45.7)	37 (42.5)	27 (50.9)	0.332
DCB	76 (54.3)	50 (57.5)	26 (49.1)	0.332
Lesion length, mm	20.1±5.9	20.6±5.8	19.8±6.2	0.763
Mean balloon used	2.6±0.7	2.6±0.8	2.6±0.7	0.967
Maximal balloon pressure, atm	16.3±2.8	16.4±2.7	16.1±2.9	0.540
Mean balloon diameter, mm	3.1±0.5	3.0±0.5	3.1±0.6	0.651
Mean balloon length, mm	14.9±2.6	14.6±2.4	15.2±2.8	0.187
DCB diameter, mm	3.2±0.4	3.1±0.4	3.2±0.4	0.229
DCB length, mm	24.2±5.6	24.4±5.6	23.7±5.6	0.605
DES diameter, mm	3.0±0.5	3.0±0.5	3.0±0.5	0.570
DES length, mm	23.6±6.7	23.6±6.9	23.5±6.6	0.935
Procedural time, min	82.9±29.6	85.5±31.5	78.9±26.1	0.203
Contrast medium used, mL	230±60	230±65	230±52	0.952

*, in-stent restenosis pattern was defined as per Mehran's classification. Data are presented as n (%) and mean ± standard deviation. PMI, periprocedural myocardial injury; LAD, left anterior descending artery; RCA, right coronary artery; LCX, left circumflex artery; RVD, reference vessel diameter; DS, diameter stenosis; MLD, minimal lumen diameter; DES, drug eluting stent; DCB, drug-coated ballon.

Table 3 OCT findings in different groups

Variables	Total (n=140)	non-PMI (n=87)	PMI (n=53)	P value
Qualitative				
Homogeneous	34 (24.3)	25 (28.7)	9 (17.0)	0.116
Heterogeneous	105 (75.0)	62 (71.3)	43 (81.1)	0.191
ISNA	82 (58.6)	47 (54.0)	35 (66.0)	0.162
LRP	82 (58.6)	47 (54.0)	35 (66.0)	0.162
Intra-stent plaque rupture	67 (47.9)	35 (40.2)	32 (60.4)	0.021
TCFA-like pattern	32 (22.9)	19 (21.8)	13 (24.5)	0.713
Calcification	59 (42.1)	37 (42.5)	22 (41.5)	0.906
Peri-strut microvessels	49 (35.0)	26 (29.9)	23 (43.4)	0.104
Intra-intima microvessels	59 (42.1)	28 (32.2)	31 (58.5)	0.003
Macrophage	20 (14.3)	15 (17.2)	5 (9.4)	0.191
Cholesterol crystal	25 (17.9)	14 (16.1)	11 (20.8)	0.485
Malapposition	20 (14.3)	10 (11.5)	10 (18.9)	0.237
Thrombus				
Red	33 (23.6)	22 (25.3)	11 (20.8)	0.540
White	52 (37.1)	31 (35.6)	21 (39.6)	0.636
Quantitative				
RVA (proximal), mm^2	8.37±2.31	8.08±2.21	8.84±2.40	0.057
RVA (distal)	4.92±2.08	5.10±2.11	4.62±2.01	0.184
AS, %	78.2 (75.3, 82.8)	79.8 (76.3, 83.5)	78.0 (74.9, 81.1)	0.675
MLA, mm^2	1.82±0.73	1.75±0.69	1.93±0.78	0.127
Mean lipid arc, °	159.5±51.3	158.6±48.9	163.9±54.6	0.266
Lipid length, mm	8.8±2.9	7.8±2.6	9.5±3.2	0.302
Lipid index*	1,468±826	1,316±676	1,618±980	0.063
Mean stent diameter, mm^2	2.91±0.50	2.92±0.52	2.89±0.48	0.778
Mean stent area, mm^2	6.88±2.38	6.96±2.51	6.77±2.21	0.707

Data are presented as n (%), mean ± standard deviation, and median (interquartile range). *, lipid length multiplied with mean lipid arc. OCT, optical coherence tomography; PMI, periprocedural myocardial injury; ISNA, in-stent neoatherosclerosis; LRP, lipid-rich plaque; TCFA, thin-cap fibroatheroma; RVA, reference vessel area; AS, area stenosis; MLA, minimal lumen area.

follows: (I) the incidence of PMI after PCI for ISR was high (approximately 37.9%); (II) the prevalence of intra-intimal microvessels and intra-stent PR was higher in patients with PMI than in those without PMI; (III) multivariable logistic regression analysis showed that intra-intimal microvessels and intra-stent PR were independently associated with PMI.

Strengths and limitations

This study indicated that the neointimal characteristics identified by OCT between patients with PMI and non-PMI were different. This may provide a way to prevent PMI. While this has several limitations. First, this study was a retrospective single-center study. There were quite a few

Table 4 Predictors of PMI by multivariate analysis

Variables	OR	95% CI	P value
Age, years	0.964	0.925–1.005	0.088
Homogeneous	0.898	0.564–1.761	0.138
Heterogeneous	1.527	0.568–3.769	0.229
ISNA	2.026	0.209–9.694	0.543
LRP	0.445	0.041–4.879	0.508
Peri-strut microvessels	0.874	0.360–2.122	0.767
Intra-intima microvessels	3.193	1.280–7.966	0.013
Intra-stent plaque rupture	2.124	1.153–4.732	0.035
MLD, mm	0.818	0.039–7.179	0.697
MLA, mm^2	1.709	0.422–6.919	0.453
Mean lipid arc, °	0.937	0.854–1.029	0.172
Lipid length, mm	1.036	0.943–1.146	0.486
Lipid index	2.655	0.988–5.433	0.053
Mean balloon length, mm	1.048	0.901–1.219	0.543

PMI, periprocedural myocardial injury; OR, odds ratio; CI, confidence interval; ISNA, in-stent neoatherosclerosis; LRP, lipid-rich plaque; MLD, minimal lumen diameter; MLA, minimal lumen area.

patients with missing hs-cTnT data after revascularization. Therefore, a selection bias could not be excluded. Second, the sample size of this study was limited. Therefore, a future large-scale study is warranted. Third, the skill level or the image identification during operation between different interventional cardiologists may influence PMI. Thus it was difficult to investigate the relationship between operation and PMI. Lastly, this was an observational study and all these patients were not followed up for long periods, which was not sufficient to detect differences in prognostic value according to the presence or absence of intra-intimal microvessels and intra-stent plaque rupture.

Comparison with similar researches and explanations of findings

PMI has mainly been reported in patients with stable CAD after PCI. Owing to the lack of scientific data, the definition of PMI is based mainly on expert consensus opinions, and its prognostic relevance remains unclear (4,20). The incidence of PMI in different studies varied based on the cardiac biomarkers and definitions used (5-8). In a patient-level pooled analysis, the incidence of PMI based on the definition according to the 4th universal definition of myocardial infarction was 52.8% (5). A retrospective study (11) investigated the effect of increasing neointimal heterogeneity and neoatherosclerosis on the incidence of PMI in patients with ISR. Their results showed that the incidence of hs-cTnT-based PMI was approximately 30%, which was similar to our finding (37.9%). These discoveries indicated that the relevant occurrence of PMI was not only in native vessel but also in ISR lesion.

Studies on the association between neointimal characteristics and PMI occurrence after PCI for ISR have been extremely limited (11,21,22). Lee *et al.* (22) retrospectively analyzed the relationship between neointimal characteristics and the occurrence of PMI [defined as creatine kinase-MB (CK-MB) >99th percentile URL] in 125 patients with ISR lesions who underwent elective PCI and pre-PCI OCT examination. They found that neoatherosclerosis and TCFA were independent predictors of PMI incidence. Additionally, Kimura *et al.* (21) investigated the relationships between neointimal tissue characteristics and PMI occurrence (defined as peak hs-cTnT value during the 24 h following PCI >5×99th percentile URL) in 72 stable angina pectoris patients with ISR lesions who underwent OCT and coronary angioscopy (CAS). They found that PMI lesions had a higher prevalence of OCT defined TCFA

and CAS-derived intensive yellow neointimas than those lesions without PMI. In the multivariable logistic regression analysis, CAS-derived intensive yellow neointima was an independent predictor of PMI. Nano *et al.* (11) investigated the relationships between neointimal characteristics and the PMI occurrence in 128 patients with ISR lesions by using OCT. However, the author reported no association between the neointimal characteristics and the occurrence of PMI. In the present study, the incidence of intra-intimal microvessels and intra-stent PR was higher in patients with PMI than in those without PMI (58.5% *vs.* 32.2%, P=0.003; 60.4% *vs.* 40.2%, P=0.021, respectively). Moreover, in multivariable logistic regression analysis, intra-intimal microvessels and intra-stent PR were deemed to be independent predictors for PMI.

According to previous studies, intimal microvessels were associated with plaque vulnerability and instability and were mostly involved in the development and progression of coronary plaques (23-25). Nishida *et al.* (23) investigated the relationships between microvessels and the tissue characteristics of plaques in 44 patients with stable angina pectoris who underwent OCT. The author reported that the greater the luminal volume of the microvessels, the higher the incidence of the necrotic/lipidic tissue within the plaques. Kitabata *et al.* (26) found that the presence of microvessels detected using OCT was significantly associated with the incidence of TCFA and higher high-sensitivity C-reactive protein levels, indicating the importance of intraplaque microvessels involved in plaque progression. Moreover, a recent study showed that carotid plaque microvessels were correlated with the progression of coronary lesions in patients with CAD undergoing PCI (27). In this study, intimal microvessels were more common in patients with PMI than in those without PMI, which is consistent with the previous studies. Furthermore, Turu *et al.* (28) found that the intimal microvessels played a pivotal role in local inflammation within the vessel wall. Furthermore, Iguchi *et al.* (29) revealed that in patients with insulin resistance, intraplaque microvessels were associated with coronary plaque growth by increasing the number of red blood cells, thereby supplying the plaque with inflammatory cells and cytokines. Moreover, Sluimer *et al.* (30) investigated the pathophysiological study of atherosclerotic coronary arteries in 28 patients who died suddenly and were donors. They found that microvessels were thin-walled in normal and atherosclerotic arteries and that the density of microvessels was higher in advanced plaques than in early plaques.

A large number of previous studies have confirmed the relationship between PR and acute coronary syndrome (31-33). PR was more observed in elderly STEMI patients, usually with a higher prevalence of typical vulnerable plaque (34). Moreover, no-reflow phenomenon was more common in STEMI patients with PR and those with PR had a higher prevalence of microvascular injury (31). The higher transmural extent of myocardial infarction also occurred in patients with PR. Satogami and colleagues (32) investigated the association between PR and transmural extent of infarction (TEI) by combining OCT with contrast-enhanced cardiac magnetic resonance imaging. They found that the frequency of no-reflow phenomenon, distal embolization and microvascular obstruction was higher in patients with PR than those with non-PR. And greater TEI grade was associated with PR. In our study, the incidence of intra-stent PR was significantly higher in patients with PMI than those without PMI. And intra-stent PR was an independent predictor of PMI in the multivariable logistic regression analysis.

Implications and actions needed

Based on the previous studies, we reckoned that patients with ISR who have a higher incidence of neointimal microvessels accompanied with more unstable plaques and local inflammatory reactions, are prone to appear PMI after revascularization. Intra-stent PR caused distal embolization and impaired microcirculation, which may be another mechanism of PMI. Therefore, Early detection of intra-intimal microvessels and intra-stent PR is necessary for the ideal management of patients with ISR. A complete examination of the ISR lesions by using OCT may provide important information about the intimal characteristics. Furthermore, the management of microvessels intra-stent PR may provide a new strategy for the prevention of PMI.

Conclusions

In patients who underwent OCT before revascularization for ISR, the incidence of intra-intimal microvessels and intra-stent PR were higher in patients with PMI than in those without PMI. Multivariable logistic regression analysis showed that intra-intimal microvessels and intra-stent PR

were independently associated with PMI occurrence.

Acknowledgments

Funding: This study was supported by grants from the National Natural Science Foundation of China (No. 82200290), and the Science and Technology Program of the Guizhou Province (No. LC [2021] 026).

Footnote

Reporting Checklist: The authors have completed the STROBE reporting checklist. Available at https://cdt.amegroups.com/article/view/10.21037/cdt-23-390/rc

Data Sharing Statement: Available at https://cdt.amegroups.com/article/view/10.21037/cdt-23-390/dss

Peer Review File: Available at https://cdt.amegroups.com/article/view/10.21037/cdt-23-390/prf

Conflicts of Interest: All authors have completed the ICMJE uniform disclosure form (available at https://cdt.amegroups.com/article/view/10.21037/cdt-23-390/coif). The authors have no conflicts of interest to declare.

Ethical Statement: The authors are accountable for all aspects of the work in ensuring that questions related to the accuracy or integrity of any part of the work are appropriately investigated and resolved. The study was conducted in accordance with the Declaration of Helsinki (as revised in 2013). The study was approved by the Ethics Committee of the Affiliated Hospital of Zunyi Medical University [No. ZMU (2022)1-177] and individual consent for this retrospective analysis was waived.

References

1. Madhavan MV, Kirtane AJ, Redfors B, et al. Stent-Related Adverse Events >1 Year After Percutaneous Coronary Intervention. J Am Coll Cardiol 2020;75:590-604.
2. Kastrati A, Cassese S. In-Stent Restenosis in the United States: Time to Enrich its Treatment Armamentarium. J Am Coll Cardiol 2020;76:1532-5.
3. Neumann FJ, Sousa-Uva M, Ahlsson A, et al. 2018 ESC/EACTS Guidelines on myocardial revascularization. Eur Heart J 2019;40:87-165.
4. Thygesen K, Alpert JS, Jaffe AS, et al. Fourth Universal Definition of Myocardial Infarction (2018). Circulation 2018;138:e618-51.
5. Silvain J, Zeitouni M, Paradies V, et al. Procedural myocardial injury, infarction and mortality in patients undergoing elective PCI: a pooled analysis of patient-level data. Eur Heart J 2021;42:323-34.
6. Zeitouni M, Silvain J, Guedeney P, et al. Periprocedural myocardial infarction and injury in elective coronary stenting. Eur Heart J 2018;39:1100-9.
7. Ndrepepa G, Colleran R, Braun S, et al. High-Sensitivity Troponin T and Mortality After Elective Percutaneous Coronary Intervention. J Am Coll Cardiol 2016;68:2259-68.
8. Ndrepepa G, Braun S, Cassese S, et al. Prognostic Value of High-sensitivity Troponin T After Percutaneous Coronary Intervention in Patients With Stable Coronary Artery Disease. Rev Esp Cardiol (Engl Ed) 2016;69:746-53.
9. Kang MG, Kang Y, Jang HG, et al. Coronary artery calcium score in predicting periprocedural myocardial infarction in patients undergoing an elective percutaneous coronary intervention. Coron Artery Dis 2018;29:589-96.
10. Hoshino M, Yonetsu T, Murai T, et al. Multimodality coronary imaging to predict periprocedural myocardial necrosis after an elective percutaneous coronary intervention. Coron Artery Dis 2018;29:237-45.
11. Nano N, Aytekin A, Ndrepepa G, et al. Periprocedural myocardial injury according to optical characteristics of neointima and treatment modality of in-stent restenosis. Clin Res Cardiol 2022;111:827-37.
12. Diagnosis and classification of diabetes mellitus. Diabetes Care 2014;37 Suppl 1:S81-90.
13. Shrank WH, Barlow JF, Brennan TA. New Therapies in the Treatment of High Cholesterol: An Argument

to Return to Goal-Based Lipid Guidelines. JAMA 2015;314:1443-4.
14. Inker LA, Astor BC, Fox CH, et al. KDOQI US commentary on the 2012 KDIGO clinical practice guideline for the evaluation and management of CKD. Am J Kidney Dis 2014;63:713-35.
15. Lal BK, Kaperonis EA, Cuadra S, et al. Patterns of in-stent restenosis after carotid artery stenting: classification and implications for long-term outcome. J Vasc Surg 2007;46:833-40.
16. Tearney GJ, Regar E, Akasaka T, et al. Consensus standards for acquisition, measurement, and reporting of intravascular optical coherence tomography studies: a report from the International Working Group for Intravascular Optical Coherence Tomography Standardization and Validation. J Am Coll Cardiol 2012;59:1058-72.
17. Otsuka F, Byrne RA, Yahagi K, et al. Neoatherosclerosis: overview of histopathologic findings and implications for intravascular imaging assessment. Eur Heart J 2015;36:2147-59.
18. Tian J, Ren X, Vergallo R, et al. Distinct morphological features of ruptured culprit plaque for acute coronary events compared to those with silent rupture and thin-cap fibroatheroma: a combined optical coherence tomography and intravascular ultrasound study. J Am Coll Cardiol 2014;63:2209-16.
19. Jia H, Abtahian F, Aguirre AD, et al. In vivo diagnosis of plaque erosion and calcified nodule in patients with acute coronary syndrome by intravascular optical coherence tomography. J Am Coll Cardiol 2013;62:1748-58.
20. Moussa ID, Klein LW, Shah B, et al. Consideration of a new definition of clinically relevant myocardial infarction after coronary revascularization: an expert consensus document from the Society for Cardiovascular Angiography and Interventions (SCAI). J Am Coll Cardiol 2013;62:1563-70.
21. Kimura S, Sugiyama T, Hishikari K, et al. Impact of optical coherence tomography- and coronary angioscopy-assessed neointimal tissue characteristics on occurrence of periprocedural myonecrosis in patients with in-stent restenosis. Int J Cardiovasc Imaging 2016;32:1483-94.
22. Lee SY, Hong MK, Shin DH, et al. Optical coherence tomography-based predictors for creatine kinase-myocardial band elevation after elective percutaneous coronary intervention for in-stent restenosis. Catheter Cardiovasc Interv 2015;85:564-72.
23. Nishida T, Hiro T, Takayama T, et al. Clinical significance of microvessels detected by in vivo optical coherence tomography within human atherosclerotic coronary arterial intima: a study with multimodality intravascular imagings. Heart Vessels 2021;36:756-65.
24. Xie Z, Hou J, Yu H, et al. Patterns of coronary plaque progression: phasic versus gradual. A combined optical coherence tomography and intravascular ultrasound study. Coron Artery Dis 2016;27:658-66.
25. Uemura S, Ishigami K, Soeda T, et al. Thin-cap fibroatheroma and microchannel findings in optical coherence tomography correlate with subsequent progression of coronary atheromatous plaques. Eur Heart J 2012;33:78-85.
26. Kitabata H, Tanaka A, Kubo T, et al. Relation of microchannel structure identified by optical coherence tomography to plaque vulnerability in patients with coronary artery disease. Am J Cardiol 2010;105:1673-8.
27. Han Y, Ren L, Fei X, et al. Association between Carotid Intraplaque Neovascularization Detected by Contrast-Enhanced Ultrasound and the Progression of Coronary Lesions in Patients Undergoing Percutaneous Coronary Intervention. J Am Soc Echocardiogr 2023;36:216-23.
28. Turu MM, Slevin M, Matou S, et al. C-reactive protein exerts angiogenic effects on vascular endothelial cells and modulates associated signalling pathways and gene expression. BMC Cell Biol 2008;9:47.
29. Iguchi T, Hasegawa T, Otsuka K, et al. Insulin resistance is associated with coronary plaque vulnerability: insight from optical coherence tomography analysis. Eur Heart J Cardiovasc Imaging 2014;15:284-91.
30. Sluimer JC, Kolodgie FD, Bijnens AP, et al. Thin-walled microvessels in human coronary atherosclerotic plaques show incomplete endothelial junctions relevance of compromised structural integrity for intraplaque microvascular leakage. J Am Coll Cardiol 2009;53:1517-27.
31. Soeda T, Higuma T, Abe N, et al. Morphological predictors for no reflow phenomenon after primary percutaneous coronary intervention in patients with ST-segment elevation myocardial infarction caused by plaque rupture. Eur Heart J Cardiovasc Imaging 2017;18:103-10.
32. Satogami K, Ino Y, Kubo T, et al. Impact of Plaque Rupture Detected by Optical Coherence Tomography on Transmural Extent of Infarction After Successful Stenting in ST-Segment Elevation Acute Myocardial Infarction. JACC Cardiovasc Interv 2017;10:1025-33.

33. Saia F, Komukai K, Capodanno D, et al. Eroded Versus Ruptured Plaques at the Culprit Site of STEMI: In Vivo Pathophysiological Features and Response to Primary PCI. JACC Cardiovasc Imaging 2015;8:566-75.
34. Fang C, Dai J, Zhang S, et al. Culprit lesion morphology in young patients with ST-segment elevated myocardial infarction: A clinical, angiographic and optical coherence tomography study. Atherosclerosis 2019;289:94-100.

Cite this article as: Shen Y, Wang X, Gu N, Liu Z, Rong J, Shen C, Zhang W, Chen P, Deng Y, Deng C, Ma S, Zhao Y, Zhao R, Shi B. Association between periprocedural myocardial injury and neointimal characteristics in patients with in-stent restenosis: an optical coherence tomography study. Cardiovasc Diagn Ther 2024;14(1):5-17. doi: 10.21037/cdt-23-390

Supplementary

Table S1 Predictors of PMI by univariable and multivariate analysis

Variables	Univariate logistic regression			Multivariate logistic regression		
	OR	95% CI	P value	OR	95% CI	P value
Age[a], years	0.975	0.941–1.009	0.152	0.964	0.925–1.005	0.088
Sex	0.789	0.312–1.994	0.616			
Hypertension	0.669	0.333–1.342	0.258			
Diabetes mellitus	0.647	0.280–1.494	0.308			
Dyslipidemia	1.484	0.696–3.166	0.307			
Smoking	0.914	0.461–1.810	0.796			
Stroke	0.814	0.144–4.603	0.816			
CKD	1.372	0.606–3.107	0.448			
Previous MI	1.135	0.535–2.407	0.741			
Triglyceride, mmol/L	1.194	0.901–1.582	0.217			
TC[b], mmol/L	1.023	0.792–1.322	0.860			
HDL-C[b], mmol/L	1.552	0.567–4.244	0.392			
LDL-C[b], mmol/L	0.979	0.691–1.389	0.907			
Homogeneous	0.507	0.216–1.192	0.119	0.898	0.564–1.761	0.138
Heterogeneous	1.734	0.756–3.977	0.194	1.527	0.568–3.769	0.229
ISNA	1.655	0.815–3.358	0.163	2.026	0.209–9.694	0.543
LRP	1.655	0.815–3.358	0.163	0.445	0.041–4.879	0.508
TCFA-like pattern	1.163	0.519–2.605	0.713			
Calcification	0.959	0.480–1.916	0.906			
Peri-strut microvessels	1.799	0.883–3.663	0.106	0.874	0.360–2.122	0.767
Intra-intima microvessels	2.269	1.463–6.025	0.003	3.193	1.280–7.966	0.013
Intra-stent plaque rupture	2.264	1.127–4.548	0.022	2.124	1.153–4.732	0.035
Red thrombus	0.774	0.340–1.759	0.541			
White thrombus	1.185	0.586–2.397	0.636			
Cholesterol crystal	1.366	0.569–3.280	0.486			
LAD	1.115	0.539–2.305	0.770			
RCA	0.814	0.366–1.814	0.615			
LCX	1.723	0.526–5.650	0.369			
DS[c], %	0.968	0.916–1.024	0.262			
MLD[d], mm	2.202	0.727–6.671	0.163	0.818	0.039–7.179	0.697
AS[c], %	0.997	0.949–1.048	0.910			
MLA[e], mm^2	1.425	0.889–2.285	0.141	1.709	0.422–6.919	0.453
Mean lipid arc, °	2.383	0.893–4.264	0.091	0.937	0.854–1.029	0.172
Lipid length[d], mm	1.786	0.823–2.671	0.153	1.036	0.943–1.146	0.486
Lipid index	3.352	1.741–5.433	0.038	2.655	0.988–5.433	0.053
DES	1.403	0.707–2.787	0.333			
DCB	0.713	0.359–1.415	0.333			
Aspirin	0.736	0.342–1.581	0.432			
P2Y12 inhibitor	0.822	0.394–1.712	0.600			
β-blocker	0.996	0.429–1.313	0.993			
Statin	1.019	0.411–2.524	0.968			
NT-proBNP[f], pg/mL	1.383	0.785–3.267	0.259			
Lesion length, mm	1.897	0.783–3.662	0.286			
Mean balloon used	0.99	0.625–1.568	0.967			
Maximal balloon pressure, atm	0.962	0.849–1.089	0.537			
Mean balloon diameter, mm	1.165	0.604–2.245	0.649			
Mean balloon length, mm	1.094	0.957–1.250	0.189	1.048	0.901–1.219	0.543
procedural time, mm	0.992	0.980–1.004	0.204			
contrast medium used, mL	1.001	0.995–1.006	0.951			

[a], OR for age was calculated for each 1-year increase; [b], OR for total cholesterol, triglyceride, LDL-C and HDL-C were calculated for each 1.0 mmol/L increase; [c], OR for DS and AS was calculated for each 1% increase; [d], OR for MLD was calculated for each 1 mm increase; [e], OR for MLD was calculated for each 1 mm^2 increase; [f], OR for NT-proBNP was calculated for each 1 pg/mL increase.

https://dx.doi.org/10.21037/cdt-23-390